LIFT AT HIGH ANGLE OF ATTACK OF A FUSELAGE-DELTA WING CONFIGURATION WITH CANARD LATERAL JETS

Mihai Neamtu, *Dr. Ing.*
Institutul National de Cercetari Aerospatiale"Elie Carafoli"-INCAS, Romania

Keywords: *Lateral Jets, Fluid Canard, High Lift, Vortex Lift, Wing-Fuselage*

Abstract

The paper presents experimental results obtained at the INCAS blow down wind-tunnel on a fuselage-delta wing model with jets blown laterally from inside the fuselage through thin slots located upstream the wing (Canard position). The model, equipped with a six component internal balance and Kulite pressure transducers and designed to allow different configuration / blowing slots arrangements, was tested at low wind tunnel Mach numbers.

The tests were made at constant incidence, with blowing intensity sweeping from high to low pressures, by freely discharging the air supplied from a battery of high-pressure cylinders.

The experimental results evidenced a complex interaction between the Canard jets and the fuselage-delta wing configuration, producing at high angle of attack (28°-34°) and high blowing rates, an important lift increase of up to 20%..

1   Introduction

The complex aerodynamic interaction produced by a pair of jets, blown laterally from inside the fuselage through thin slots located upstream of a fuselage mounted delta wing, was experimentally studied at the INCAS 1.2m×1.2m blow-down wind tunnel (W-T) starting from 1996 (see *Acknowledgments*). The location of the jets suggests the name of "Canard like lateral jets" or simply "Canard jets". Alternately the assembly of the two lateral jets can be referred to as "Fluid Canard".

Previously, the idea of this study was mentioned in an ICAS'96 paper [1], mainly devoted to the background aerodynamic theory of the lateral jets **blown from the wing tips** of a general wing-fuselage combination. In particular, this general theory includes the simpler case of the fuselage alone with lateral jets, interesting directly the interaction process occurring in the case of wing-fuselage configuration with fluid Canard.

As for the wing-fuselage combinations with **wing-tip** lateral jets, extensive treatment of the general theory and its applications can also be found in [2], and also in [3] to [7].

2   General presentation of test conditions.

2.1 The test model and blowing arrangement.

Figure 1 shows schematically the wing-fuselage test model with jets blown laterally from inside the fuselage through thin slots located upstream of the Delta wing.

The model is composed of a cropped Delta wing, a vertical tail (not shown in the figure) and a cylindrical fuselage with a circular cross section terminating by an AGARD nose. The dimensions are evident from the figure. Other relevant features follows bellow.

The Delta wing is generated from symmetrical circular-arc sections of constant relative thickness (5%), the leading and trailing edges mainly resulting as the intersection of the upper and lower arcs with a small adjustment radius.

The fuselage has three modules, namely the main, the jet and the AGARD nose modules.

The main module supports the wing, allowing it to be mounted in five vertical combined with three axial positions. Also, the main module houses a 2-inch internal balance TASK MK XXVI. The balance provides three axial positions for the main module of which only one was actually used.

The jet module, located between the main and the nose modules, has a build in blowing chamber composed of an upstream entry portion having a conical variation of the cross section, and a cylindrical settling chamber (60 mm inside diameter) with two opposite thin slots.

The air is supplied from a battery of up to 24 high-pressure cylinders via two flexible hoses continued by metallic pipes (10 mm inside diameter) that are connected to the upstream end of the blowing chamber.

When entering the blowing chamber, the air is dispersed into small jets by passing through a perforated cone. A mixing process occurs homogenizing the flow, while the air mean velocity decreases drastically, due to the conical increase of the cross section diameter, until the settling chamber is reached. Both processes ensure a uniform pressure in the settling chamber, where the velocities of the air are supposed to be very low. In the same time, the pressure obtained in the settling chamber is 10 to 12 times lower then the pressure in the high-pressure cylinders, making a pressure reducing devise unnecessary for the needs of the present paper tests.

The two thin slots are located in the mid plane of the jet settling chamber. The maximum chord of the slot, c_j, is 130 mm. By conveniently covering segments of the slot one can adjust both the chord and its axial position. One can also adjust the thickness of the slots, δ_j, up to about 2.5 mm.

In particular, these adjustment capabilities allow the Canard jets to be located exactly in front of the wing, i.e. with the trailing edge (T.E.) of each slot coinciding with the leading edge (L.E.) of the corresponding wing root section. This specific location was selected for the tests reported in the present paper

2.2 The wind tunnel.

The INCAS 1.2m×1.2m blowdown wind tunnel was build in cooperation with the Canadian company DSMA and is of the same type as the IAR (NAE) 1.5m×1.5m blowdown wind tunnel in Ottawa. The tunnel is pressurized for high Reynolds numbers capabilities and runs at Mach numbers from 0.1 to 3.5. It has a flexible nozzle and a variable diffuser that can be shaped to the necessary configuration for subsonic, transonic and supersonic operation. A removable transonic section must be inserted between the flexible nozzle and the variable diffuser for transonic operation.

Three test chambers are available, of which one, with a square cross section of 1.2m×1.2m and solid walls, is represented by the downstream end of the flexible nozzle and is used for subsonic and supersonic Mach numbers lower than 0.6 or higher than 1.6 respectively. *This test section was the one used for the present tests.*

The other two test chambers are used as inserts into the transonic section. The 3-D insert, having a square cross section of nearly 1.2m×1.2m and four perforated walls with variable porosity, operates in the Mach number range 0.6-1.6. The 2-D insert has a cross section of 0.48m×1.2m, top and bottom perforated walls and operates in the Mach range 0.6-1.05.

A 3 tank battery stores 2000 cubic meter of air compressed by two Ingersoll Rand compressors at a pressure of up to 20 bars. During the pump-up the tanks are isolated from the rest of the tunnel by a shut-off valve that must be opened one minute before the run, when the control of the air is transferred to a pressure regulating valve (PRV). The blowdown test is realized by emptying the air from the tanks into a settling chamber preceding the flexible nozzle and the rest of the tunnel. The pressure in the settling chamber is automatically controlled by the PRV during the entire blowdown sequence.

All control parameters of the blowdown sequence, including PRV, are in their turn controlled by a process computer, that also

controls the data acquisition system (see bellow).

A strut-sting assembly, situated in the vertical symmetry plane of the variable diffuser, and located at its upstream end, immediately behind the test chamber, supports the model, via internal balance. A parallelogram system transforms the vertical translation of the strut into the sting rotation around a central point of the test chamber. This way the model remains in the center of the tunnel while changing its incidence.

In regular cases, when straight stings are used, the incidence ranges from -15° to +24°. *In our case, the model was supported by a 10°-bent sting, allowing the incidence to range from -5° to +34°.*

2.3 The measuring system and primary data processing

The measuring system consists in a set of measuring devices monitored by a fast computer controlled data acquisition system.

There are two categories of measurements, one grouping the parameters that are common to all types of tests, including the wind tunnel operation parameters and the other for the specific parameters needed for each particular test.

The parameters of first category, relevant for the present paper, and the corresponding location and measuring devices are as follows:

p_0 -total pressure, W-T settling room,
       CEC 200 psia electro-manometer;
p -static pressure, test section,
       CEC 60 psia electro-manometer;
T_o -total temperature, W-T settling room,
       thermo-rezistence;
α_s -sting incidence, encoder;

The relevant measurements belonging in the second category (see also figure 1) are as follows:

P_{j0} -total pressure, jet settling chamber,
       Kulite 200 psia pressure transducer;
p_j -static pressure, jet slot lip,
       Kulite 100 psia pressure transducer;

Also belonging in this category are the three forces and three moments measured by the six- component internal balance.

All the parameters are read nearly simultaneously in sequences of 16 channels (including some other parameters that were not mentioned), at 50 ms intervals. The recorded electrical signals are corrected for offsets and tares and converted in physical units using the calibration characteristics of the measuring devices.

The transformed data are grouped in sets of 25 and reduced, by statistical analysis, to mean values of the measured parameters for well defined time-intervals. The standard data processing includes also corrections for the usual tunnel errors.

2.4 The experimental procedure

The wind-on tests were performed with the model maintained at a preset constant incidence over the entire run. The data acquisition system starts reading the data immediately after the signal "test pressure established". These initial data correspond to the model in the absence of the jet blowing. Three seconds latter, the jet blowing system is activated and the air from the high-pressure cylinders is discharged freely through the slots into the main flow, while the measuring system continues the acquisition of the data.

It is interesting to note that the time variation of the blowing pressure can be controlled conveniently by the number of high-pressure cylinders connected to the jet blowing battery. By reducing the number of cylinders one obtains a more rapid decrease of the blowing pressure, resulting in a shorter run. In our case a 6-cylinder battery resulted in about 30-35 seconds of the total run duration.

2.5 The jet momentum exhaust rate.

The exhaust speed V_j and the density of the jet air at the slot ρ_j are controlled by the slot geometry and by the blowing conditions.
The exhaust jet momentum rate J is given by the expression:

$$J = \rho_j \delta_j c_j V_j^2 = \gamma \delta_j c_j p_j M_j^2 \qquad (1)$$

…where γ=1.4 (for air) is the ratio of specific heats.

To evaluate the validity of the above expression for our specific pressure measuring conditions, a direct measurement of J, using the internal balance, was made in the same time with the blowing pressure measurements, during special jet blowing tests in wind-off conditions. The measuring arrangement is as shown in figure 2.

As one can see, J can be calculated either by using eq. (1) and the measured blowing pressures or by using the force F, as given by the internal balance (see figure 2), and the following simple expression, based on the momentum theorem, considering the two plates to be parallel:

$$2 \cdot J = F \cdot 38/117$$

The comparison between the two calculations for critical exhaust conditions *(Mj=1)* in the case c_j=130 mm, δ_j=1 mm was plotted in the self-explained chart of figure 3.

The small differences obtained for high or low jet momentum are mainly produced by the deformations of the measuring apparatus due to the inherent flexibility of sting-balance assembly and by jet-flow conditions on the two plates for non-parallel position. One must take into account that the two plates were pre-set in a slightly convergent position before starting the jets, so only the mid portion of the chart, were the differences are minimum, corresponds to nearly parallel plates.

These tests confirm that the errors, if any, are of the order of several percents.

Denoting by ρ_∞ and U_∞ the main flow reference density and velocity respectively, the jet momentum rate coefficient C_j or simply the jet coefficient can be defined by the following formula:

$$C_j = \frac{2J}{\rho_\infty U_\infty^2 c_j^2} \qquad (2)$$

…or, in terms of pressures and Mach numbers:

$$C_j = 2 \frac{p_j}{p_{j0}} \cdot \frac{\delta_j}{c_j} \cdot \frac{p_{j0}}{p_\infty} \cdot \frac{M_j^2}{M_\infty^2} \qquad (3)$$

For critical or *super*critical exhaust conditions M_j=1 and the pressure ratio p_j/p_{j0}=0.5283, so (3) simplifies to

$$C_j = 1.0566 \frac{\delta_j}{c_j} \cdot \frac{p_{j0}}{p_\infty} \cdot \frac{1}{M_\infty^2} \qquad (3')$$

…while for *sub*critical conditions we must use (3), whith the exhaust Mach number given by

$$M_j^2 = \frac{2}{\gamma - 1} \cdot \left[\left(\frac{p_{j0}}{p_j} \right)^{\frac{\gamma-1}{\gamma}} - 1 \right]$$

As a consequence, with γ=1.4 one obtains for C_j

$$C_j = \frac{10}{M_\infty^2} \frac{\delta_j}{c_j} \frac{p_{j0}}{p_\infty} \frac{p_j}{p_{j0}} \left[\left(\frac{p_{j0}}{p_j} \right)^{0.2857} - 1 \right] \qquad (3'')$$

It is important to note that the above definition of the jet coefficient C_j, using $(c_j)^2$ as reference surface, is in accordance with the definition used in (1), (2) and (4) to (8), where the general aerodynamic theory of lateral jets was presented.

3 Experimental results and discussion

In accordance with the experimental procedure, the experimental results are represented by the variation of the usual aerodynamic coefficients (lift C_L, drag C_D and pitching moment C_m) with respect to the jet coefficient C_j for different test conditions. The reference parameters for these coefficients were the wing surface S_A= *0.1476 m²* and the mean aerodynamic chord C_{MA}= *0.277m* while the reference point for the pitching moment was at 25% of the mean aerodynamic chord.

The experimental program included tests at Mach numbers 0.2, 0.3 and 0.4, for different relative positions of the slot and wing and for different values of the slot chord and thickness. Not all these tests were successful or resulted in expected effects, but all helped learning the experimental technique and founding better combinations.

Among the most encouraging experimental results, mainly demonstrating the capacity of the Fluid Canard to produce a lift increase of wing-body configurations at high angle of attack are those presented in figure 4. These tests were performed at M=0.2 for a jet exhaust slot having a 90-mm chord and thickness of 1 mm. The jet exhaust conditions at the slot were critical ($M_j=1$). The wing was in its most advanced axial position, in the same plane as the jet exhaust slot, the T.E. of the slot coinciding with the L.E. of the root section of the wing.

As one can see, at angles of attack equal or higher than 28° an important increase of lift coefficient is evident, going up to 20% for jet coefficients increasing to about 0.85.

Also evident are the accompanying drag and pitching moment increases, suggesting that the Fluid Canard can be useful not only to improve the lifting capacity of the aircraft at low speeds, but also its low speed maneuvering performances (especially in fly by wire conditions).

At low angles of attack, the Fluid Canard influence on the overall aerodynamic coefficients is very low so these results are not interesting for the present paper.

Even at high angles of attack, for low jet coefficients, the results indicate a small decrease of the lift coefficient rather than positive effects. This aspect has a theoretical importance suggesting a three-way interaction between the Canard jets and the fuselage-delta wing configuration, as follows:

(1) a favorable direct interaction between the jets and fuselage, representing a limit situation of the general theory described in [2];

(2) a down / up-wash effect of the jet wake on the wing, that can also be treated by using the general theory presented in [2] to calculate the induced perturbations on the wing. The favorable effect of the up-wash perturbations occurs only for sufficiently powerful blowing;

(3) a favorable vortex lift type effect of the Canard jets upon the delta wing, similar to close-coupled (solid) Canard-wing interaction. However, the flow produced at the tip of the jet sheet is the result of a more complex, first of all turbulent, mixing process between the jet filaments and the vortex flow generated by the interaction with the main flow.

As a result of above considerations, the small decrease of the lift *for low jet coefficients* at high angles of attack, can be explained by a dominant down-wash effect of the Canard jets affecting the near-fuselage region of the wing, while the favorable effects are still small.

The favorable effects produced by the direct fuselage-jet, up-wash and vortex lift type interactions, become dominant only for jet coefficients higher than *0.5*, as evident from figure 4.

References

[1] Mihai Neamtu, "Aerodynamic assessment of lateral jet sheets and their influence on wing-body combinations for some blowing arrangements". 20th *ICAS Proceedings*, Sorrento, Italy, Vol. 1, pp 446-456, 1996

[2] M. Neamtu, *"Contributii la studiul jeturilor laterale si a aplicatiilor acestora"*, *Ph.D. Thesis*, 1980

[3] E. Carafoli, "The influence of lateral jets, simple or combined with longitudinal jets, upon the wings lifting characteristics*"*, *Proc. of the 3rd ICAS*, 1962

[4] E. Carafoli, N. Camarasescu, *"Noi cercetãri asupra aripilor de alungire micã cu jeturi laterale"*, *Studii si Cercetãri de Mecanicã Aplicatã*, XX, 4, 1970. English translation: *"New research on small span-chord ratio wings with lateral jets"*, NTIS, AD-733858.

[5] E. Carafoli, M. Neamtu, *"New theoretical developments on the wing with lateral jets"*, *OMMAGIO A CARLO FERRARI*, ed. univ. Levrotto and Bella, Torino, Italy, dec. 1974.

[6] E. Carafoli, M. Neamtu, *"Flow around wings with inclined lateral jets"*, *Mech. Research. Comm.*, vol. 3, no. 3, 1976.

[7] E. Carafoli, M. Neamtu, *"Aerodinamica aripilor cu jeturi laterale înclinate"*, *Studii si cercetãri de Mecanicã Aplicatã*,XXXV, 2, iun. 1976.
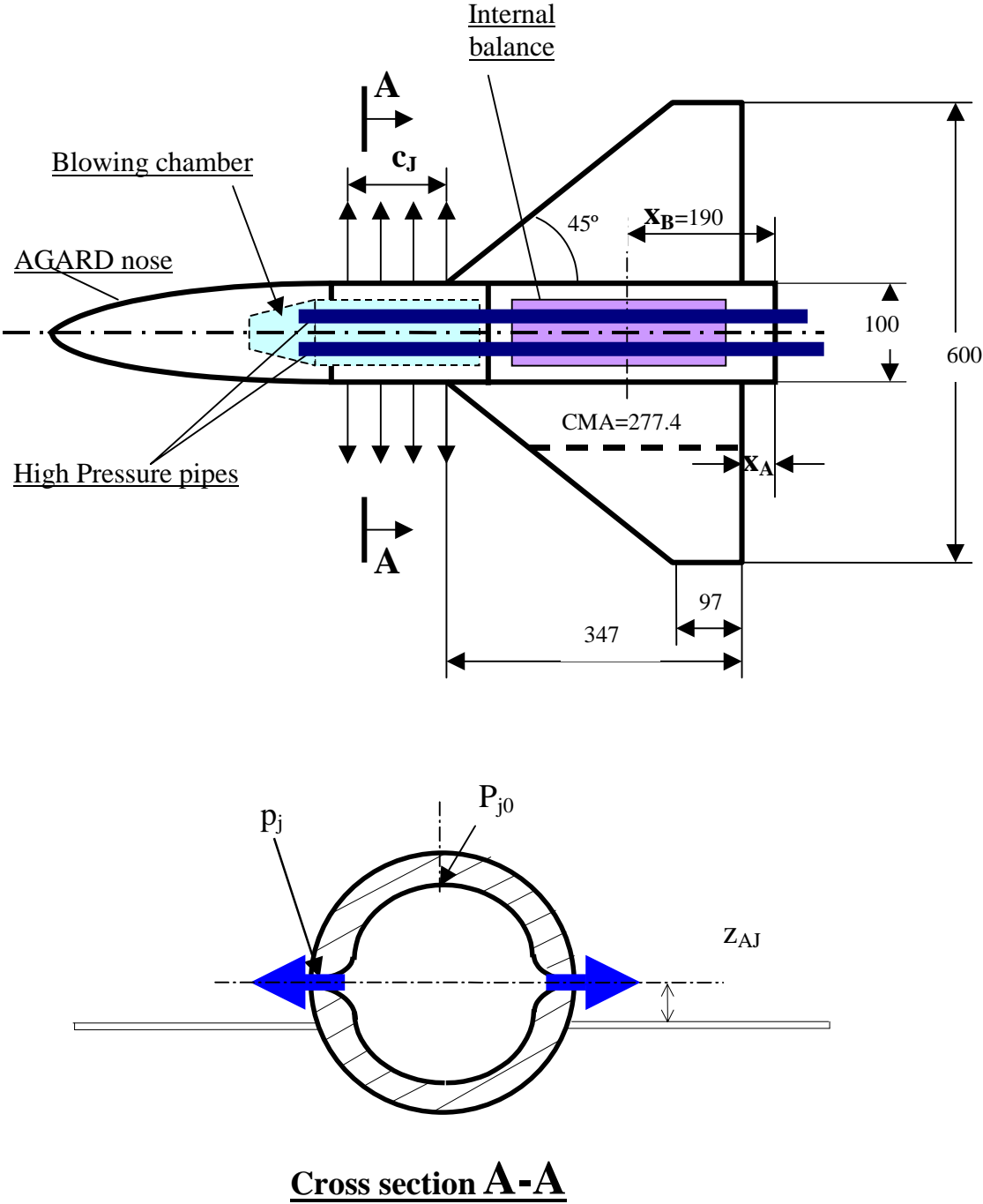
Internal
balance

A

c_J

Blowing chamber

$x_B=190$

45º

AGARD nose

100

600

CMA=277.4

High Pressure pipes

x_A

A

97

347

P_{j0}

p_j

z_{AJ}

Cross section A-A

Figure 1. Schematic of the wing-fuselage test model with Canard lateral jets
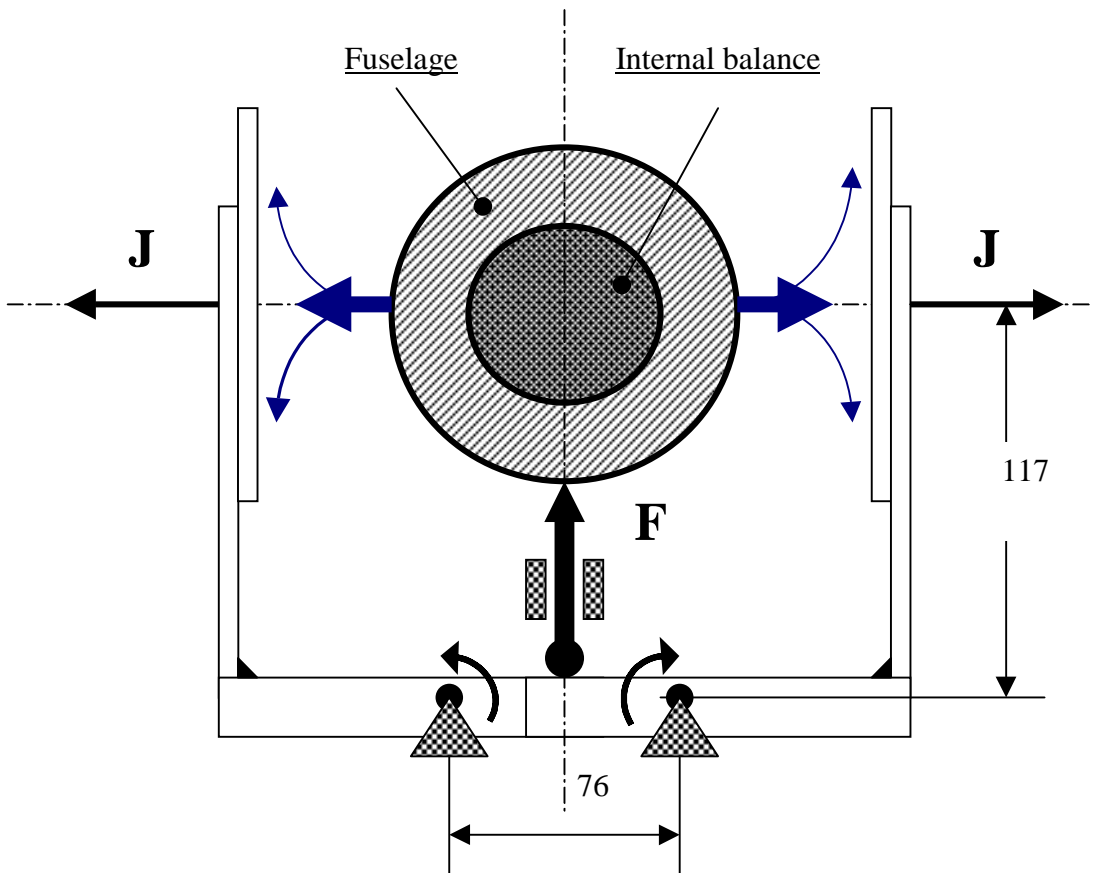
Figure 2. Schematic of the direct method for measuring the jet-
momentum using the internal balance

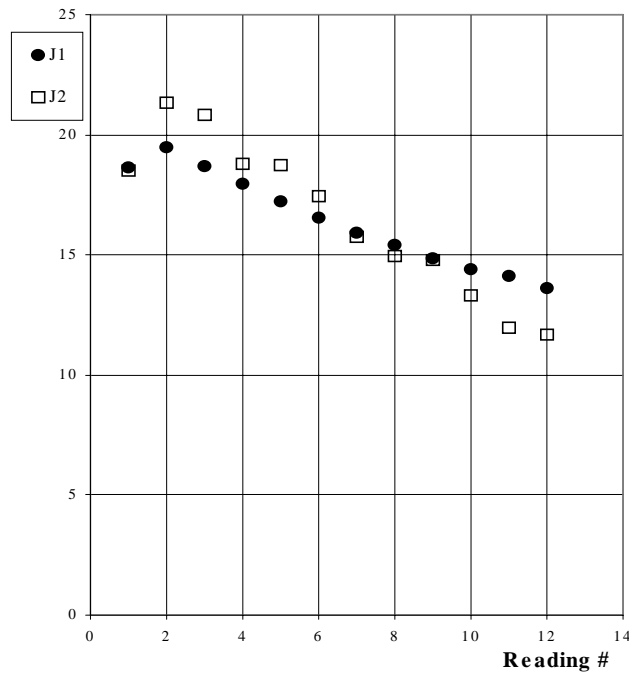Figure 3 Jet momentum calculation using the blowing pressure (J1)
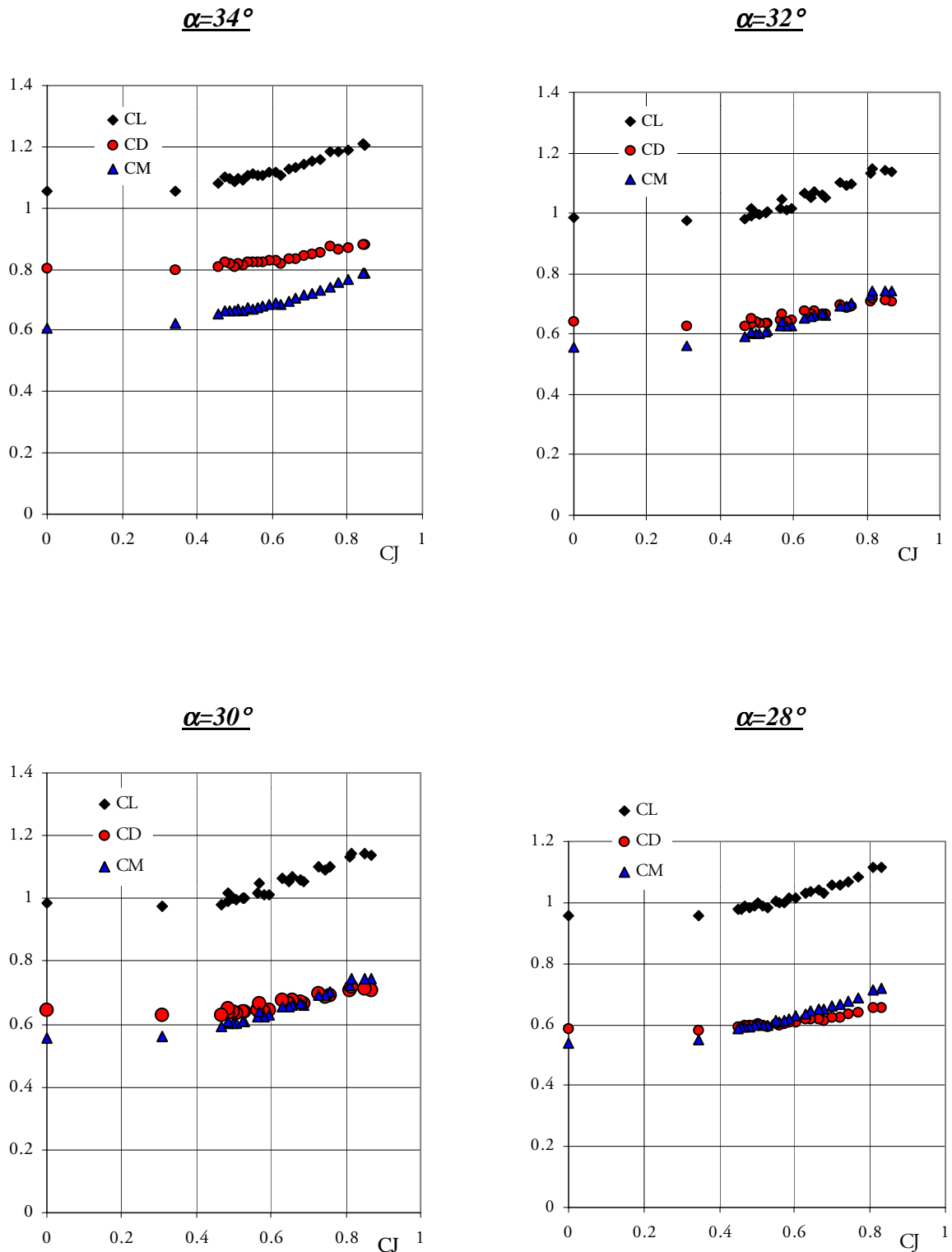and the internal balance data (J2).

Figure 4. Lift, drag and pitching moment coefficients versus jet coefficient C_j (CJ) at *M=0.2* and different incidences (*α=34°; α=32°; α=30°; α=28°*). Slot chord c_j*=90* mm, slot thickness t_j*=1* mm